Low-lying $^3P^o$ and $^3S^e$ states of Rb$^-$, Cs$^-$, and Fr$^-$

C. Bahrim[1] and U. Thumm[1,2]

[1]*J.R. Macdonald Laboratory, Department of Physics, Kansas State University, Manhattan, Kansas 66506-2601*
[2]*Institute for Theoretical Atomic and Molecular Physics, Harvard-Smithsonian Center for Astrophysics, 60 Garden Street, Cambridge, Massachusetts 02138*

Our Dirac R-matrix calculations suggest that none of the heavy alkali-metal negative ions, Rb, Cs, and Fr, has an excited bound state. Their lowest excited state appears to be a multiplet of $^3P_J^o$-shape resonances, the $J=1$ component of which was recently observed in photodetachment experiments on Cs$^-$. We analyze these $^3P_J^o$ and the $^3S^e$ excited negative ion states in partial and converged total scattering cross sections for slow electrons with incident kinetic energies below 120 meV. Our results are in excellent agreement with available experimental data. We also propose a new value for the electron affinity of Fr, provide the scattering length for electronic collisions with Rb, Cs, and Fr, and discuss the nuclear charge dependence of relativistic effects in the resonance profiles.

PACS number(s): 34.80.Dp, 34.80.Bm, 31.50.+w

I. INTRODUCTION

In the past decades, the low-lying states of negative ions have attracted wide interest for both theoreticians and experimentalists. Buckman and Clark [1] have recently reviewed this subject. Negative *alkali-metal* ions are of particular interest because of their simple structure, consisting of two electrons outside a fairly rigid (but polarizable) noble-gas-like core. In this paper we focus on the lowest-lying resonance states of the heaviest negative alkali-metal ions, Rb$^-$, Cs$^-$, and Fr$^-$, within an energy range up to 120 meV above the detachment threshold (which will be the reference energy throughout this work). For this purpose, we shall analyze the collision between a projectile electron and a neutral alkali-atom target.

For Rb$^-$ and Cs$^-$, reliable experimental results are available for the electron affinity (EA) [2] and the first excited states [1,3–5]. The negative ion of Fr is less well studied, and we are aware only of the calculations by Greene [6] for the EA and the photodetachment spectrum below the $6d$ excitation threshold. For neutral Fr, recently published energy levels and radiative transition probabilities [7], as well as theoretical atomic and core polarizabilities [8,9], provide the necessary input for the Dirac R-matrix calculations presented below.

At impact energies below the first atomic excitation threshold, precise electron-atom scattering experiments are difficult, and only a limited set of measured data is available for Rb [3,4] and Cs [3,4,10] targets. For Rb targets, electron-transmission measurements [3] have suggested a $^3P^o$ resonance below 50 meV. However, these measurements could not resolve the fine structure of this temporarily bound state of Rb$^-$. As far as we know, no previous calculations explain this finding. Very recently, photodetachment experiments on Cs$^-$ [5] have clearly shown that the Cs$^-(^3P_1^o)$ resonance exists at 8 meV above the detachment threshold. The good agreement with recent R-matrix calculations [11,12] suggests that the $J=0$ and 2 terms of the Cs$^-(^3P_J^o)$ multiplet (which are not accessible in single-photon detachment out of the negative ion ground state) are also unbound. This ends a long-lasting debate about the possible existence of a bound excited state of Cs$^-$, in agreement with the predictions of earlier Dirac R-matrix calculations [11].

II. BRIEF REVIEW OF THE DIRAC R-MATRIX THEORY

Our computations are based on the suite of relativistic Dirac R-matrix programs of Thumm and Norcross [11] that provide electron-impact scattering data within an effective two-electron model. The two active electrons (the scattered and alkali valence electron) interact with the noble-gas-like core through the semiempirical Thomas-Fermi-Dirac-Amaldi potential $V_{TFDA}(\lambda;r)$ and the potential $V_{pol}(\alpha_d,\alpha_q,r_c;r)$, which describes the induced polarization of the noble-gas-like core in response to the interaction with an outer electron. For the dipole (α_d) and quadrupole (α_q) core polarizabilities we take the following reliable data from the literature:[1] $\alpha_d=9.076$, $\alpha_q=35.41$ for Rb$^+$ [13]; $\alpha_d=15.64$, $\alpha_q=33.60$ for Cs$^+$ [14]; and $\alpha_d=20.41$ [8], $\alpha_q=127.30$ [9] for Fr$^+$. The potentials depend on the orbital and total angular momentum quantum numbers of the valence electron l and j through the length-scaling parameters λ and the adjustable core radius r_c, the latter being introduced to cut off V_{pol} close to the target nucleus where dipole and quadrupole polarizations lose their physical meaning. We determined these parameters by adjusting the computed atomic energies to the available experimental data for neutral Rb [15], Cs [15], and Fr [16], using the least-squares fitting procedure of Zhou and Norcross [14]. For Fr, the experimental database alone is insufficient for a reasonable fit of λ and r_c, and we had to add theoretical data [7]. Table I shows the values of λ and r_c for the first five lj series of levels. With these values, we find that the one-electron Dirac equation with the potential $V_{TFDA}+V_{pol}$ reproduces the lowest five atomic energy levels in each lj series of the Rb, Cs, and Fr spectra better than 1% accuracy.

---

[1]Unless stated otherwise, we use atomic units.

TABLE I. The λ and r_c parameters of the core potential for Rb, Cs, and Fr, obtained by least-squares fitting to the first five lj series of atomic levels.

Core		$s_{1/2}$	$p_{1/2}$	$p_{3/2}$	$d_{3/2}$	$d_{5/2}$
Rb^+	λ	0.949	0.999	1.003	0.985	0.928
	r_c	2.108	4.099	4.305	2.969	2.288
Cs^+	λ	1.060	1.069	1.074	1.052	1.000
	r_c	3.349	4.107	4.309	2.976	2.302
Fr^+	λ	0.985	1.020	1.023	1.029	0.983
	r_c	3.003	4.999	4.999	3.991	3.013

We describe the correlation between the two active electrons as the sum of the usual Coulomb interaction $1/|\vec{r}_1 - \vec{r}_2|$ and a dielectronic polarization potential [11] $V_{diel}(\alpha_d, \alpha_q, R_c; \vec{r}_1, \vec{r}_2)$. R_c is an adjustable cutoff parameter, that may be regarded as an effective atomic radius. V_{diel} represents the interaction between the dipole, induced in the core-electron distribution by one outer electron, with the other outer electron. We obtain $R_c = 4.679$ and 5.109 by fitting the calculated negative-ion ground-state energy to the accurate experimental EAs [2], 485.918 meV and 471.483 meV, for Rb and Cs, respectively.

No experimental EA is available for Fr. The only EA for Fr we could find in the literature is calculated by Greene [6]. This value is based on the jj-coupled eigenchannel R-matrix approach in which the Schrödinger equation is solved including a spin-orbit interaction term, but without the repulsive dielectronic correlation potential. Postulating a 10% decrease of the EA for Fr due to V_{diel}, Greene arrives at a value for the EA of 462 meV. Figure 1 shows the EAs of all alkali metals as a function of their nuclear charge Z. We find that the inclusion of V_{diel} decreases the EA by 7.7% for Rb and 9.7% for Cs. For Fr, we choose V_{diel} to induce a 10% change
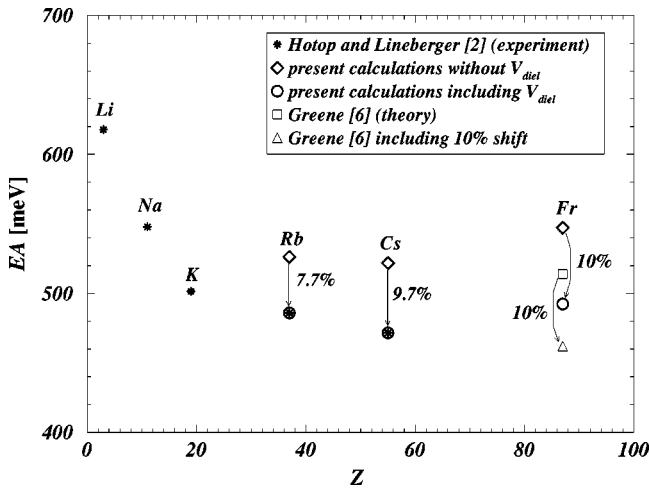

FIG. 1. Electron affinities for all alkali-metal atoms. The experimental values are taken from Ref. [2]. For Rb, Cs, and Fr, our calculated values, without the dielectronic potential V_{diel}, are also shown. For Fr we compare our calculation with the result of Greene [6].

in the calculated EA, in agreement with the assumption of Greene [6]. By omitting V_{diel}, we calculate an EA of 526.33 meV for Rb, 521.83 meV for Cs, and 547.16 meV for Fr. Shifting the negative-ion ground-state level upward by 10% results in the EA of 492.46 meV for Fr.

Lacking accurate data, we estimate the EA of Fr (492.46 meV) based on a somewhat intuitive analysis of the influence of the dielectronic polarization potential V_{diel} on the EA of heavy alkali-metal atoms and the comparison of their atomic radii. V_{diel} is attractive and strongly dominated by the dipole core polarizability term [11]. Since the dipole polarizability for Fr^+ is 31% larger than for Cs^+ and more than twice as large as for Rb^+, we assume that the inclusion of V_{diel} in the total Hamiltonian for the Fr$+e^-$ system induces an upward shift in energy for the negative-ion ground state that is at least as large as for Cs. This amounts to a lower limit for the decrease of the Fr EA due to V_{diel} of 9.7%. Our numerical tests have confirmed that the EA increases with the R_c parameter. In view of the increasing atomic size, we expect the value of R_c to increase from Rb ($Z = 37$) to Fr ($Z = 87$). This trend is in part confirmed by our cutoff radii for Rb (4.679) and Cs (5.109). By assuming that R_c for Fr is at least as large as for Cs, the inclusion of V_{diel} with $R_c = 5.109$ leads to an EA for Fr of 486.35 meV, equivalent to an upper limit for the V_{diel}-induced shift of 11.1%. In view of these rather crude estimates, we expand our confidentiality interval for the V_{diel}-induced shift in the Fr EA from [9.7%, 11.1%] to [8%, 12%]. A shift of 8% gives an EA of 503.39 meV and corresponds to $R_c = 5.903$; for a 12% shift we obtain 481.50 meV and $R_c = 4.906$. In conclusion, we estimate the EA for Fr at 492.46 meV (corresponding to a V_{diel}-induced shift of 10% and to $R_c = 5.375$) with an uncertainty of $\pm 2.2\%$ for the EA and $\pm 10\%$ for R_c.

We note in passing that our values of R_c increase with Z from Rb to Fr, whereas our fit of R_c to Greene's previously published EA for Fr (462 meV) results in $R_c = 4.066$, which is smaller than our R_c value for Rb (4.679) and does not follow this intuitive trend. We also note that, in contrast to Greene's estimated dipole core polarizability for Fr ($\alpha_d = 22$), our calculation is based on a new computed value (20.41) [8].

Our scattering calculation includes close coupling between the first five bound states of the target: $ns_{1/2}$, $np_{1/2}$, $np_{3/2}$, $(n-1)d_{3/2}$, $(n-1)d_{5/2}$ (with $n=5$ for Rb, $n=6$ for Cs, and $n=7$ for Fr). We use 28 continuum orbitals (CO) in each scattering channel. This guarantees the convergence of (partial and total) cross sections for collisions up to 2.8 eV, if part of the incompleteness in the basis of CO is compensated by including a Buttle correction [11]. The two-electron wave functions are combined as sums of antisymmetrized products of bound and continuum orbitals in a standard jj-coupling scheme, for each J^π scattering symmetry (J and π are the conserved total angular momentum and parity of the scattering system). We diagonalize the total Hamiltonian of the two-electron model system inside a sphere (the ''R-matrix sphere'') of radius $R=40$. This value is large enough so that exchange between the projectile and target electrons is negligible outside the sphere.
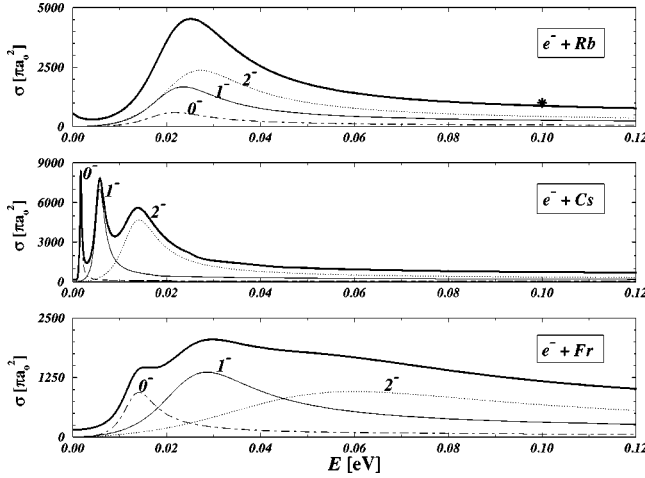
FIG. 2. Partial (thin lines) and total (thick lines) elastic cross sections for e^-+Rb, Cs, and Fr scattering below 120 meV showing the $^3P^o$-shape resonances and their fine-structure components: 0^- (dot-dashed line), $J^\pi=1^-$ (thin solid line), and 2^- (dotted line). The star at 0.1 eV shows the calculated result by Fabrikant [17].

After diagonalizing the two-electron Dirac Hamiltonian inside this finite volume, we match the ''inner-space'' solutions (given by the eigenvectors of the diagonalization) to solutions for the spatial region outside the R-matrix sphere. These ''outer-space'' solutions include channel couplings due to long-range induced dipole and quadrupole interactions. From the solutions of the matching equations for each (J,π) pair all relevant scattering information is obtained, such as the K-matrix, scattering phase shifts, partial cross sections, and negative ion states. For more details we refer to [11].

The analysis of partial cross sections and eigenphase sums $\Delta^{J\pi}(E)$ (obtained from the diagonalized K matrix) in each J^π symmetry and on a very fine mesh of scattering energies E allows us to identify scattering resonances. For an isolated resonance, $\Delta^{J\pi}(E)$ is given as the sum of a slowly varying background phase shift Δ_0 and a strongly energy-dependent resonance term $\tan^{-1}\{\Gamma/[2(E_r-E)]\}$, where Γ is the width of the resonance state. Thus $\Delta^{J\pi}$ increases by approximately π near the resonance position E_r. In order to find reliable estimates for Γ, we examined both $\Delta^{J\pi}$ and the half-maximum values of partial cross sections in the relevant J^π symmetries. The resonance positions are most accurately determined from the maximum of the derivative of $\Delta^{J\pi}$ as a function of E.

III. RESULTS AND DISCUSSION

Figure 2 shows the converged total cross sections for the elastic scattering of electrons with incident energies below 120 meV on Rb, Cs, and Fr targets, including a data point from the nonrelativistic two-state close-coupling calculation by Fabrikant [17]. Also shown are partial cross sections for odd parity and $J=0,1$, and 2 symmetries. For scattering on Rb, Johnson and Burrow [3] experimentally identified a $^3P^o$ resonance below 50 meV, but could not resolve its fine structure. Our calculation reveals that even for infinite energy

resolution, the fine structure of this resonance could not be resolved in the total cross section, because the widths of individual $^3P^o_J, J=0,1,2$ terms is significantly larger than their spacing in energy. The position of the Rb$^-$($^3P^o$) resonance in the total cross section (at 25 meV) is shifted by a few meV with respect to the J-averaged value $\bar{E}_r=\Sigma(2J+1)E_r(J)/\Sigma(2J+1)=21.8$ meV of its fine-structure terms (Table II). The resonance width in the total cross section is a little larger than the J-averaged width $\bar{\Gamma}=19.3$ meV. The influence of V_{diel} on the Cs$^-$ spectrum was previously analyzed [11] and found to shift the negative-ion ground state upward by 50 meV and the lowest excited states upward by 20 to 30 meV. In the current calculations these shifts for the $^3P^o_J$ terms amount to 15.8, 15.3, and 15.0 meV for Rb$^-$ and 30.3, 23.8, and 15.4 meV for Fr$^-$, respectively, for $J=0,1$, and 2.

For Cs targets, all fine-structure terms of the ($^3P^o$) resonance can be resolved in the total scattering cross section (Fig. 2). With respect to Fr targets, all Cs$^-$ fine-structure terms are shifted to lower energies and have significantly reduced widths (Table II). The J-averaged resonance positions and widths of the $^3P^o$ resonance of Rb$^-$ and Cs$^-$ are in good agreement with the semiempirical results of Fabrikant [18] that are based on the modified effective range theory (MERT) (Table II). For Fr, the term with the highest angular momentum ($J=2$) of the ($^3P^o$) resonance can barely be identified in the total cross section. Compared to Rb and Cs targets, the J-averaged position for Fr$^-$ is the furthest away from the detachment threshold, and the J-averaged width is the largest.

For all three heavy alkali targets, we find that the ($^3P^o$) negative ion resonance lies energetically very close to the ground state of the parent atom. These shape resonances can be interpreted as the result of a potential well, formed by the sum of the attractive short-range atomic potential and the repulsive centrifugal potential, which temporarily traps one of the outer electrons, before releasing it in a p-wave. This picture is confirmed by an eigenvector analysis of the diagonalization inside the R-matrix sphere. We find that eigenvectors corresponding to eigenvalues next to resonances in the $J^\pi=0^-,1^-$, and 2^- partial cross sections are dominated by $ns_{1/2}n'p_j$ configurations, where $n=5$ for Rb, $n=6$ for Cs, $n=7$ for Fr, and $n'\geq n$. The contributions of these configurations in Table II are obtained from their squared amplitudes.

As expected, the fine-structure splitting of the $ns_{1/2}n'p_j(^3P^o)$ negative-ion resonances increases with increasing nuclear charge. According to our results in Table II, the splitting $\Delta E_r(J,J')=E_r(J)-E_r(J')$ between the ($^3P^o_J$) terms increases with Z^4/n^3. The splittings between neighboring terms deviates most from Landé's interval rule for the Fr target ($Z=87$), but also noticeably for Rb ($Z=37$) and Cs ($Z=55$), thereby indicating the significance of relativistic effects and the breakdown of pure Russell-Sounders coupling for high-Z targets. To quantify this statement, we note that for pure Russell-Sounders coupling, the interval rule requires the constant $C=\Delta E_r(2,1)/\Delta E_r(1,0)$ to be equal to 2, whereas the values in Table II clearly deviate from this prediction by up to 20% for Fr$^-$.

TABLE II. Position E_r and width Γ for the $^3P^o$ terms of Rb$^-$, Cs$^-$, and Fr$^-$, together with the constant C (see text), the dominant jj-coupled configurations, and comparison with experimental data [3,5]. For the J-averaged resonance energies $\bar{E}_r$ and widths $\bar{\Gamma}$ MERT results [18] are included.

Ion	J^π	Dominant configurations (%)	E_r (meV) Our work	E_r (meV) Others	Γ(meV) Our work	Γ(meV) Others	$^3L_J^\pi$	C
Rb$^-$	0^-	$5sn'p_{1/2}$(95.4)	19.21		14.84		$^3P_0^o$	
	1^-	$5sn'p_{1/2;3/2}$(77.3)	20.42	<50 [a]	18.24		$^3P_1^o$	2.3
	2^-	$5sn'p_{3/2}$(95.4)	23.22		20.89		$^3P_2^o$	
	J-averaged		21.84	23 [b]	19.33	25 [b]	$^3P^o$	
Cs$^-$	0^-	$6sn'p_{1/2}$(94.7)	1.69		0.36		$^3P_0^o$	
	1^-	$6sn'p_{1/2;3/2}$(89.6)	5.53	8.0 [c]	2.67	5.0 [c]	$^3P_1^o$	1.8
	2^-	$6sn'p_{3/2}$(95.4)	12.74		8.73		$^3P_2^o$	
	J-averaged		9.11	9.5–12.6 [b]	5.78	5.7–9.1 [b]	$^3P^o$	
Fr$^-$	0^-	$7sn'p_{1/2}$(95.8)	13.21		9.40		$^3P_0^o$	
	1^-	$7sn'p_{1/2;3/2}$(79.5)	24.02		25.71		$^3P_1^o$	1.6
	2^-	$7sn'p_{3/2}$(98.3)	40.84		68.13		$^3P_2^o$	
	J-averaged		32.16		47.46		$^3P^o$	

[a]Reference [3].
[b]Reference [18].
[c]Reference [5].

Since all $^3P_J^o$ terms are within 41 meV of the detachment threshold, where the scattered electron's wave number $k = \sqrt{2E_r} \ll 1$, we would expect Wigner's threshold law [19] for scattering of partial waves with angular momenta l, $\Gamma \sim E_r^{l+1/2}$, to hold. Indeed, the resonance positions and widths listed in Table II comply with $\Gamma \sim E_r^{3/2}$, giving additional support to our correct characterization and computation of the $^3P^o$ resonances.

Since no precise value for the EA of Fr is available, the question arises, to what extent our assumed uncertainty of 2.2% in the EA (10% in cutoff radius R_c, cf. Sec. II) affects scattering cross sections and resonance parameters. In order to give a quantitative answer to this question, we have investigated the dependence of the cross section for elastic electron-Fr scattering at incident electron energies below 120 meV. This energy region covers the lowest $^3P^o$ resonance. Since higher-lying resonances tend to be less localized near the nucleus, their positions and widths are expected to depend less sensitively on R_c than the parameters for the lowest $^3P_J^o$ terms. We thus expect to obtain reasonable upper limits for the uncertainty of resonance positions and widths by solely investigating the R_c dependence of cross sections near the lowest $^3P_J^o$ terms. In Fig. 3, we compare the $^3P_J^o$ fine-structure components computed with the extreme values for R_c, 4.906 and 5.903, with results obtained by using $R_c = 5.375$, which corresponds to our estimated Fr EA of 492.46 meV. The figure shows that for $J=0$, both position and width are strongly modified by the choice of different values for R_c. This influence decreases for components with higher values of J. The positions (widths) of the $^3P_J^o$ terms in

Table II vary by 36% (60%) for $J=0$, by 14% (23%) for $J=1$, and by 5% (7%) for $J=2$, for R_c values in the interval [4.906, 5.903]. For all components, the resonance width is much more sensitive to the choice of R_c than the resonance position. Shape and magnitude of the total elastic scattering cross section are also sensitive to the choice of the R_c pa-
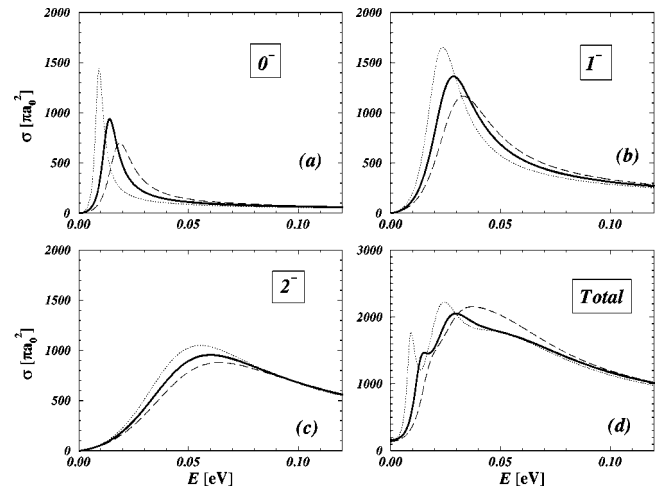

FIG. 3. The influence of the cutoff parameter R_c in the dielectronic polarization potential on partial cross sections [(a) $J^\pi=0^-$, (b) 1^-, (c) 2^-] and converged total elastic (d) cross sections for electron scattering on Fr targets. The dotted and dashed curves correspond to calculations with an R_c parameter of 5.903 and 4.906, respectively. The solid curves are the same as in Fig. 2 and correspond to calculations with $R_c=5.375$.
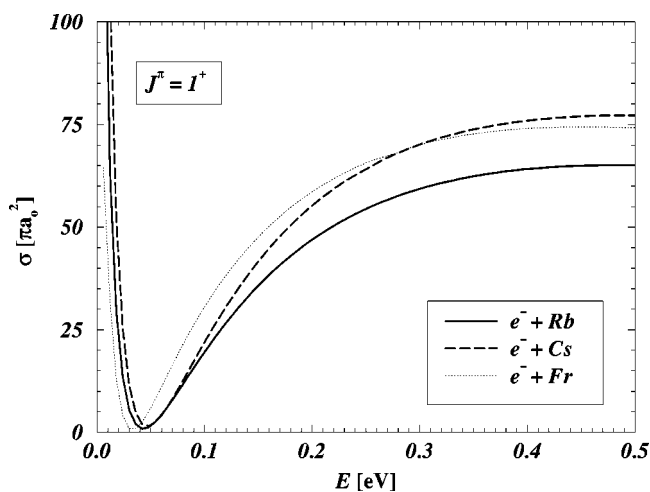
FIG. 4. The Ramsauer-Townsend minima in the $J^\pi = 1^+$ partial elastic scattering cross sections for Rb, Cs, and Fr targets.

rameter. Figure 3(d) shows that for $R_c = 5.903$, all fine-structure components of the $^3P^o$ resonance are clearly distinguishable. In contrast, for $R_c = 4.906$, the $J = 2$ component disappears in the background. Irrespective of the relatively large error bar of our estimated values for positions and widths of the Fr$^-$($^3P^o_J$) terms, our calculations clearly indicate that this state is not bound, as for the case of Cs$^-$ and Rb$^-$.

In the $J^\pi = 1^+$ symmetry we find that the lowest eigenvalue (of the diagonalization within the R-matrix sphere) corresponds to eigenvectors with more than 99% contributions from $ns_{1/2}n's_{1/2}$ configurations (where $n = 5$ for Rb, 6 for Cs, and 7 for Fr, and $n' \geq n+1$). The lack of any other eigenvalues within a few 10 meV makes the designation of the $^3S^e_1$ excited state unambiguous. We find Ramsauer-Townsend (RT) minima in the partial cross sections at 41 meV for Rb, 46 meV for Cs, and 32 meV for Fr (Fig. 4).

Due to the dominant s-wave character, the $^3S^e_1$ state differs from a typical shape resonance. A simple interpretation of the $^3S^e$ excited state is given by expanding the s-wave phase shift in powers k [18,19], $\tan \delta_{l=0} = -Ak - [\pi\alpha/3]k^2 + O(k^3)$, where A is the scattering length and α is the atomic polarizability. For negative A and $k = (-3A/\alpha)/\pi$, the phase

shift vanishes, leading to the RT minimum, the position of which moves to higher energy for increasing atomic polarizabilities. Our Dirac R-matrix results yield $A = -13$ for Rb, -17 for Cs, and -12 for Fr and are a little smaller in magnitude than the MERT results [18] of Fabrikant (-16.9 for Rb and -22.7 for Cs). Thus, for negative scattering lengths, the large polarizability of the heavy alkali-metal atoms [8] leads to the formation of a potential well that supports the $^3S^e$ excited state. Our calculations reveal that this state is a virtual state, since (i) it is s-wave dominated and (ii) we do not find the usual change by π of the eigenphase sum near the RT minimum.

IV. SUMMARY AND OUTLOOK

We have investigated the $^3P^o$ and $^3S^e$ low-lying excited states of Rb$^-$, Cs$^-$, and Fr$^-$, by analyzing elastic electron scattering on the parent alkali-metal atoms at low impact energies. As far as we know, this is first calculation for $e^- +$ Fr scattering. In view of the very instructive recent photodetachment experiments on Cs$^-$ [5], we hope that our results stimulate new electron scattering and photodetachment experiments that probe the electronic structure of Rb$^-$ and Fr$^-$. Of particular interest would be photodetachment experiments that scrutinize our calculated values for the positions and widths of the $^3P^o_1$ term. More details on the spectra of Rb$^-$, Cs$^-$, and Fr$^-$, up to an energy of 2.8 eV above the detachment threshold, will be presented in a forthcoming paper.

[1] S.J. Buckman and Ch.W. Clark, Rev. Mod. Phys. **66**, 539 (1994).

[2] H. Hotop and W.C. Lineberger, J. Phys. Chem. Ref. Data **14**, 731 (1985).

[3] A.R. Johnson and P.D. Burrow, J. Phys. B **15**, L745 (1982).

[4] A.R. Johnson and P.D. Burrow, Phys. Rev. A **51**, 406 (1995).

[5] M. Scheer, J. Thogersen, R.C. Bilodeau, C.A. Brodie, H.K. Haugen, H.H. Andersen, P. Kristensen, and T. Andersen, Phys. Rev. Lett. **80**, 684 (1998).

[6] C.H. Greene, Phys. Rev. A **42**, 1405 (1990).

[7] E. Biemont, P. Quinet, and V. Van Renterghem, J. Phys. B **31**, 5301 (1998).

[8] A. Derevianko, W.R. Johnson, M.S. Safronova, and J.F. Babb,

Phys. Rev. Lett. **82**, 3589 (1999).

[9] A. Derevianko and W.R. Johnson (private communication).

[10] W. Gehenn and E. Reichert, J. Phys. B **10**, 3105 (1977).

[11] U. Thumm and D.W. Norcross, Phys. Rev. Lett. **67**, 3495 (1991); Phys. Rev. A **45**, 6349 (1992); **47**, 305 (1993).

[12] K. Bartschat, J. Phys. B **26**, 3595 (1993).

[13] W.R. Johnson, D. Kolb, and K-N. Huang, At. Data Nucl. Data Tables **28**, 333 (1983).

[14] H.L. Zhou and D.W. Norcross, Phys. Rev. A **40**, 5048 (1989).

[15] C.E. Moore, *Atomic Energy Levels*, Natl. Bur. Stand. (U.S.) Circ. No. NSRDS-NBS 35 (U.S. GPO, Washington, D.C., 1971), Vols. II and III.

[16] A. Arnold *et al.*, J. Phys. B **23**, 3511 (1990); J.E. Simsarian, A. Ghosh, G. Gwinner, L.A. Orozco, G.D. Sprouse, and P.A. Voytas, Opt. Lett. **21**, 1939 (1996).

[17] I. Fabrikant, Phys. Lett. **58A**, 21 (1976).

[18] I. Fabrikant, J. Phys. B **19**, 1527 (1986); Comments At. Mol. Phys. **32**, 267 (1996).

[19] L.D. Landau and E.M. Lifschitz, *Quantum Mechanics. Non-relativistic Theory* (Pergamon Press, Oxford, 1977).